



Area Estimation of the Mandelbrot Set Using Monte-Carlo Methods

[illegible]

5284STSI6Y

2 Background

The relevance of the Mandelbrot set as a testing ground for Monte Carlo techniques lies in its notorious geometric complexity. Infinitely rich in spatial features, its structure cannot be explored without the use of sophisticated simulation tools. The application of Monte Carlo sampling as means to capture its spatial extent carries the benefit that it is generally a problem-agnostic approach which harnesses the potentials of probabilistic search without the need for detailed information about the problem. The method can nonetheless be enhanced by different variance reduction techniques, in particular through stratification and by constraining the search space to the regions of highest variance.

Mandelbrot Set The Mandelbrot set is a mathematical object of great importance in the study of Complex Systems and Chaotic Dynamics[1]. It is defined as the set of complex numbers which do not diverge beyond toward infinity when iterated through a recursive function. While it is proven that the set is compact and connected[2], its boundary exhibits extreme complexity, with self-similar structures occurring on various scales of magnification (Fig. 1) in patterns which elude simple analytical predictions. This abnormal behaviour is underlined by the fact that the Hausdorff dimension of the boundary is 2[3], which is an entire integer above its topological dimension. These indications hint on the issue that while there may exist a limit for the area of the Mandelbrot set, the problem of quantifying it with absolute precision poses a great challenge given finite computational resources.

Various attempts to approach this include narrowing down the possible area bounds[4, 5], using lattice-based sampling with escape-time algorithms[6] and approximating the shape and bounds of the constituent regions of the set[7]. Despite this, there is no established ground-truth value for the area up to date, even though different estimations point to a number a few thousands above 1.5[8].

Monte-Carlo Integration Monte Carlo methods implement probabilistic approaches to obtain a measure of an integral by sampling the problem space with randomly generated input points. In particular, a hit-or-miss Monte Carlo integration applies well to the estimation of the area of two-dimensional geometries where the boundary is not discrete or well-defined by analytical methods. By relying on the effect of chance, the uniform distribution of the coordinates and the presumably continuous range of their possible values, this method guarantees that any region in space can hypothetically be sampled, as opposed to deterministic approaches such as pixel counting, and thus a sufficiently accurate approximation can be obtained given enough samples.

The performance of a specific Monte Carlo implementation can be measured by the relationship between the variance of the results and the amount of samples necessary to obtain a certain accuracy, i.e. how fast the estimates converge to a mean value with the increase of the sample size. The most basic scheme involves generating pseudo-random sample point coordinates from a uniform distribution. While this approach is straightforward to implement, various techniques can be used to reduce the variance of its output. One such technique involves stratified sampling[9], which introduces a spatial structure to the sampling space and thereby neutralizes the effect of local density variance which may occur in purely random methods. Relating to the problem of area estimation, this provides a balance between stochastic exploration and a regularly space-filling spread of the samples. The three special Monte Carlo variants explored in the current research: Latin Hypercube (LHS) and Orthogonal Sampling[10], and our own proposed Adaptive Grid Rank sampling are representative of such approaches.

3 Methods

The stochastic simulation framework consists of several distinct modules. First, a population of samples is generated using an appropriate *Sample Generator*. Initialised as Cartesian coordinates, the samples are converted into complex numbers and are used to evaluate their inclusion in the set in a *Mandelbrot Iterator* module. The resulting escape times are then fed into an *Area*

Estimator function and finally the area estimates undergo various types of statistical analysis in a *Statistical Testing and Plotting* module.

The framework is programmed in Python and presented in a Jupyter notebook together with the documented series of experiments. The procedures make extensive use of the *NumPy* library for enhanced data array management, *Pandas* for logging data relevant for statistics and *Matplotlib* for plotting visual results. The methods implemented in the simulation modules are outlined below.

Evaluating the Mandelbrot set The object of interest in the current research is the quadratic implementation of the Generalized Mandelbrot set, which includes the complex numbers c for which the sequence described by the following recursive formula does not diverge:

$$z_{n+1} = z_n^2 + c \quad (1)$$

To compute the inclusion status, a number z is calculated for a finite number of iterations indicated by i ($n \leq i$), starting with $z_0 = c$. If the magnitude $|z_n|$ exceeds a threshold value of 2 at any $n < i$ the sequence is considered divergent and therefore not part of the Mandelbrot set. In that case the number of iterations n at that point are returned. If the number of iterations reaches i , the complex number is considered to be in the Mandelbrot set and i is returned. The returned iteration number is commonly denoted as *escape time*.

Area of the Mandelbrot set The test for inclusion in the set consists of a binary check whether a point has reached i at termination without diverging. The general procedure to compute the area estimate A follows the following formula:

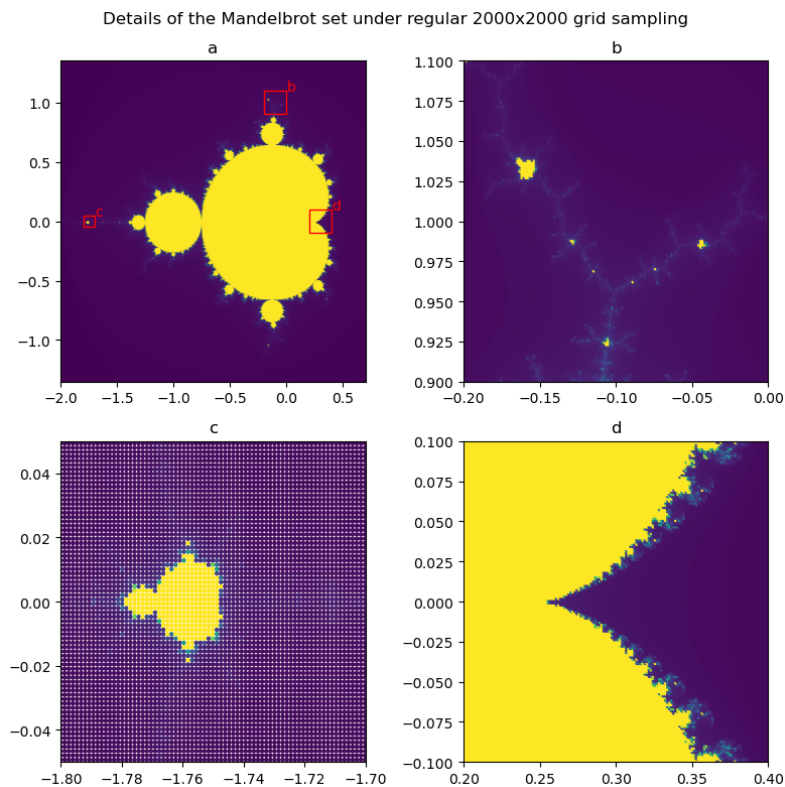


Figure 1: Magnified views of the Mandelbrot boundary illustrating self-similar formations and the difficulty in capturing details with discrete sampling and a finite iteration count. Points that did not diverge beyond $|z| = 2$ are marked in yellow, while the others are coloured from green to purple based on their escape time.

$$A = \frac{s_{in}}{s} \times A_{rect} \quad (2)$$

where s_{in} is the number of sample points that fall inside the shape, s is the total number of sample points generated for the realisation and A_{rect} is the area of the rectangle enclosing the shape, given by the intervals $[x_{min}, x_{max}]$ and $[y_{min}, y_{max}]$ along each coordinate axis of the complex plane.

A major difficulty in determining the true area of the Mandelbrot set is due to the fact that the true number of iterations until divergence ($|z| > 2$) is unknowable unless an infinite i is permitted. We therefore test multiple threshold i values and for each one assume inclusion if the sequence has not diverged before reaching it. This fails to capture sequences with a higher escape time than our chosen i which would be excluded from the set. A ground-truth reference area A_M is therefore unknown. To make an estimate of it with the available computational resources, we choose a maximum number of iterations $i = 1500$ and highest sample size $s = 16200$ which yield our best estimate $A_{i,s}$. The reference value is obtained by taking the mean $\bar{A}_{i,s}$ of the resulting areas from 1000 stochastic realisations. As the quality of the result may vary depending on the sampling method, $\bar{A}_{i,s}$ is determined separately for each method, the estimates being defined as $\bar{A}_{i,s(PR)}$, $\bar{A}_{i,s(LHS)}$, $\bar{A}_{i,s(O)}$ and $\bar{A}_{i,s(RG)}$ for Pure Random, LHS, Orthogonal and Grid Rank Sampling respectively.

To compare the convergence rate of sampling methods as s and i increase, we fix either of the parameters to its maximum value and incrementally increase the other. As the outline of the set changes its shape at different escape time limits, the variation of i aims to indicate the value towards which the area converges as the detail of the Mandelbrot set becomes more defined. With the highest definition fixed, the sample size is varied to illustrate the change in precision of the sampling method. The metric chosen to indicate this is the error calculated as:

$$error = \bar{A}_{i,s(method)} - A_{j,s(method)} \quad (3)$$

where $j < i$ and $A_{j,s(method)}$ is the area result from a single realisation. The results from both parameter variation studies are presented in two plots indicating the sample averages and the confidence intervals.

Useful Properties of the Mandelbrot set In order to narrow down the sampling space and be able to acquire higher precision with smaller sample sizes, some heuristics based on inherent properties of the Mandelbrot set can be taken into consideration. For instance, it is easily noticeable that the set exhibits symmetry along the $Re(c)$ axis. This can be confirmed by the observation that the conjugate \bar{z} of a complex number z can be expressed as:

$$\bar{z} = Re(z) - Im(z)i \quad (4)$$

If we denote the real component of z_n as a and the factor of its imaginary component as b , under transformation through the Mandelbrot function in Equation 1 the complex number and its conjugate become:

$$z_{n+1} = (a + bi)^2 + a + bi = a^2 + a - b^2 + (2ab + b)i \quad (5)$$

$$\bar{z}_{n+1} = (a - bi)^2 + a - bi = a^2 + a - b^2 - (2ab + b)i \quad (6)$$

Since $Im(\bar{z}_n) = -Im(z_n)$ at every n , this suggests that the magnitude of the iterated number is invariant under symmetry transformation along the real axis. Using the knowledge of this symmetry, it can be stated that it is sufficient to sample only the positive imaginary half of the complex plane, knowing that the other half would have an equal area. The total area is thus calculated as twice the area estimate for the half-plane.

Using a conservative modification of findings in literature[11], we define the limits of a bounding square of the Mandelbrot set as $x \in [-2, 0.7]$ and $y \in [-1.35, 1.35]$ (or, in case of observing only the half-space, $y \in [0, 1.35]$). This guarantees that all potential members of the set are within the observation space. Naturally, some points with a distance higher than 2 from the origin are included in the rectangle, but these are discarded from the set at the first iteration step so a pre-filtering is not deemed necessary.

Pure Random Monte Carlo Sampling In our implementation of the basic Monte Carlo sampling, we draw 2 random numbers, x and y , from a random uniform distribution, scaled to the sampling interval, using the `numpy.random.uniform` method. The y coordinate is transformed to the imaginary domain by multiplying with i and is then combined with x into a complex number c , which is passed to the Mandelbrot function following the logic of the simulation modules. This is also the baseline approach for the more advanced sampling methods, the difference being in spatially stratified structure which they add to the scheme. When generating multiple sampling populations for a range of parameters in a specific sampling scheme, an incrementally increased seed value is taken for each realisation.

Latin Hypercube Sampling The principle of Latin Hypercube Sampling implemented in our algorithm is based on the following steps. (1) Each axis of the sampling space is subdivided in $N = s$ equal intervals. (2) A random permutation of size N of each set of intervals is taken without replacement. (3) The shuffled x and y intervals are combined into 2D-intervals. (4) The pure random sampling procedure is applied to each 2D-interval using a single sample per interval. The result guarantees that no more than a single sample will be placed in the same 2D-interval and that furthermore every row and column in the grid of intervals will contain at most one sample point. This imposes a spatial constraint on the otherwise probabilistic generation of samples.

Orthogonal Sampling A further level of stratification is added in the Orthogonal Sampling method. This approach assumes that each sample occupies a cell in a superimposed grid of size $N \times N$, $N = \sqrt{s}$. To keep the distribution of samples as even as possible, the following measures are taken. (1) A prototypical sub-grid of size $N_{sub} \times N_{sub}$ is constructed. As every cell of the $N \times N$ super-grid will be subdivided into such sub-grids, this is thought of as an initial map of a cell's coordinate space. (2) An s/N_{sub} number of LHS-like interval permutations of size N_{sub} is taken on the prototypical sub-grid. This results in a total of $N_{sub} \times s/N_{sub} = s$ 2D-intervals. (3) Discarding the hierarchical order of the 2D-intervals, one more permutation is taken over the entire set of s intervals to produce better mixing. (4) A uniform random sample is taken on each 2D-interval. (5) Each sample is translated from the prototypical sub-grid to a sub-grid inside of a different cell on the $N \times N$ super-grid.

This results in a form of *distributed* LHS sampling where the permuted points do not occupy the same interval but are rather spread out to different super-grid cells. It is therefore guaranteed that the points are allocated within regular strata and at the same time are unlikely to coincide with each other along the rows and columns of the sub-grid. It is important to note that due to the specifics of steps 2 and 3 our version of the method imposes more relaxed constraints than some examples in literature which completely eliminate the possibility of coincidence along the columns and the rows[10].

A constraint arising from this method is that the number of samples either needs to be a power of two so it can be spread over a square grid, or be of the form $2x^2$ in case only half of the square region is sampled. Furthermore, N_{sub} needs to be chosen such that it is a divisor of \sqrt{s} and each dimension is divided in a round number of intervals. For this, a procedure calculates all the divisors of \sqrt{s} and takes the value closest to the median, i.e. producing sub-grids of medium density. This excludes prime numbers, which would either yield sub-grids or super-grids of a single cell. This constraint on the sample sizes is transferred to the other sampling strategies for the sake of comparison.

Two-stage Adaptive Grid Sampling To explore further possibilities for improving the convergence rate, an extension of these methods is explored which varies the sampling density locally within the cells of a superimposed grid, taking into consideration the rate of escape in these cells. This works by performing two sampling stages with a specified size ratio. First, a coarse Orthogonal Sampling is performed and the samples are grouped evenly in larger square strata. The points undergo evaluation with Mandelbrot iteration counts i_1 and i_2 . The values for these iteration counts are picked at 5% and 50% of the maximum i . At each of these iteration counts the escape time of each sample is measured and divided by the corresponding iteration count.

These measures are averaged per grid cell, resulting in two values per grid cell which could be interpreted as the average probability for a sample to belong to the Mandelbrot set at the two stages. The absolute difference between these values indicates how much this probability has changed between the two time moments. This signifies whether the observed region is in the definite core of the set or far outside of it, in case there was no change, or if it is encompassing the boundary, a region which constantly changes with an increase of iterations.

This difference is used to create a ranking of the strata in the second stage by linearly ranking each grid cell and deriving a new sample size per cell, with a baseline sample size equal to the previous sample size per grid and the rest of the sampling budget spread based on the ranking. In the second sampling stage, LHS is performed inside each grid cell with different density and is used to calculate the area. As the first batch of samples is not iterated to the full extent, these are not counted in the final sampling budget responsible for the area estimation.

Statistical Testing of Area Error Convergence To quantitatively compare the convergence rates of different methods, we employed a pairwise two-sample T-test to determine if there were statistically significant differences in their mean errors. In addition, we utilized a pairwise F-test to assess whether the variances in error across the methods were equivalent. These statistical tests were applied to various sample sizes (denoted as s) and iteration counts (i), with the methods being compared in pairs. The null hypothesis for the two-sample T-test posits that the means of the two sample groups are equal, while the null hypothesis for the F-test asserts that their variances are equal. The p-value obtained from these tests quantifies the likelihood of observing a result as extreme as, or more extreme than, the one in the sample, under the assumption that the null hypothesis is true. The alpha level, predefined by the researcher, is the threshold for rejecting the null hypothesis. A p-value smaller than the alpha level signifies that the null hypothesis should be rejected in favor of the alternative hypothesis, which states that means are unequal in case of the T-test and variances are unequal in case of the F-test.

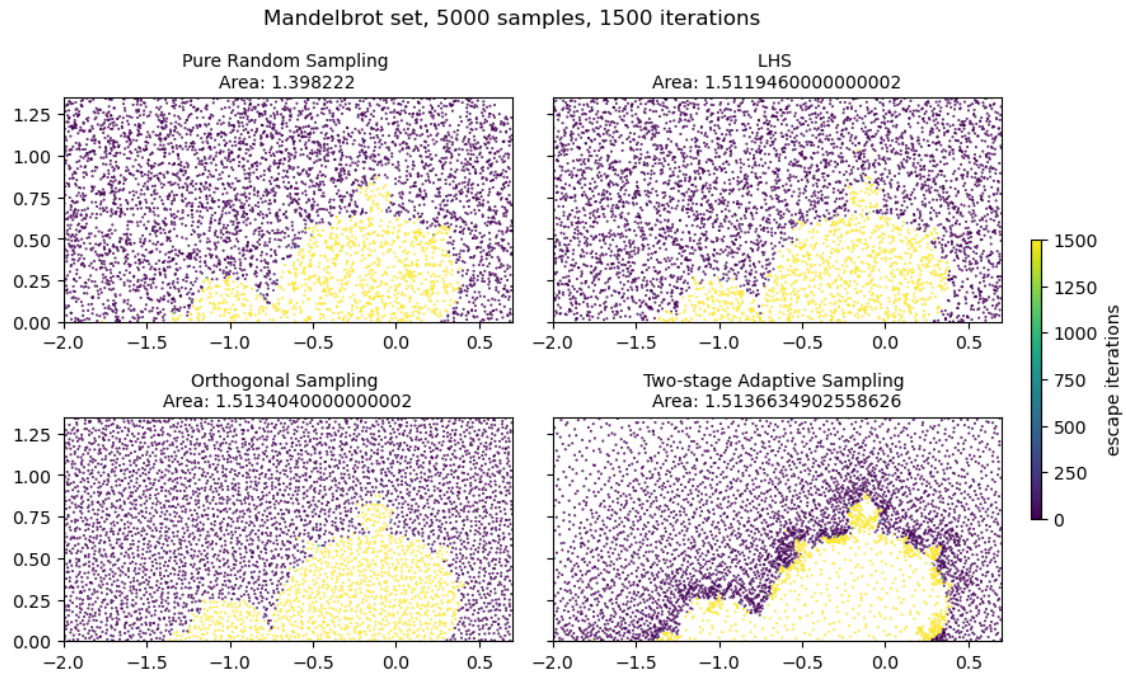


Figure 2: Examples of the four sampling methods with their resulting area estimates from a single stochastic realisation.

4 Results

The setup for the stochastic experiments involves the exploration of four methods: Pure Random Sampling, LHS, Orthogonal Sampling and the proposed adaptive technique. As a preliminary test, a scatterplot is produced from the outcome of a single sample draw (Fig. 2). After that, a range of $i \in [20, 1500]$ and a range of $s \in [200, 16200]$ are discretised with respect to the method constraints and all parameter configurations are tested in 40 simulation runs per configuration. Leveraging the symmetry property (only observing the positive half-plane) results in higher accuracy with the same sampling budget.

Next the results of the area estimation using different sampling methods are compared by showing the convergence rates of area error as s and i increase, respectively. Either of the parameters is fixed in turn, the other being incremented so isolated effects of the parameter on the Area can be observed across simulation runs.

The comparison of convergence area to mean area using maximum iterations and sample size is depicted in Figure 3, as outlined in Equation 3. This figure features shaded regions indicating a 95% confidence interval. On the left, we observe a marked decline in area estimation as iterations increase, particularly up to 110 samples. This trend levels off between 500 and 1000 iterations, a pattern that remains consistent across all methods. The right subplot illustrates a reduction in variance for each method as the sample size expands, aligning with predictions of the Central Limit Theorem. Notably, Orthogonal Sampling demonstrates the quickest convergence towards the maximum area estimate, maintaining this efficiency even at lower sample sizes. In terms of method comparisons, Orthogonal Sampling exhibits the lowest variability in both overall and mean error, followed closely by Adaptive Grid rank sampling. Latin Hypercube Sampling (LHS) shows slightly more variability, and random sampling presents the highest level of variability. However, there is some ambiguity in the overlap of 95% confidence intervals, particularly between orthogonal and adaptive grid sampling methods. To address this, T-tests and F-tests were conducted for pairwise comparisons, providing a statistical evaluation of the differences in mean and variance across methods at various increments of iteration and sample size.

The quantity tested is the Area error as defined in (3). For each setting of i and s respectively, cross sectional pairwise two-sided T-Test and F-test were done at the $\alpha = 0.05$ level. Figure 4 depicts the results of increasing increments of iterations with sample size at max (16200), while Figure 5 depicts the results for increasing increments of sample sizes with iterations fixed at max (1500). The y-axis depicts which methods are tested pairwise. The cross sectional sample obtained consists of the number of runs per setting for each method (so these cross sectional samples have size of 40 per method, so that two samples of size 40 are tested against each other).

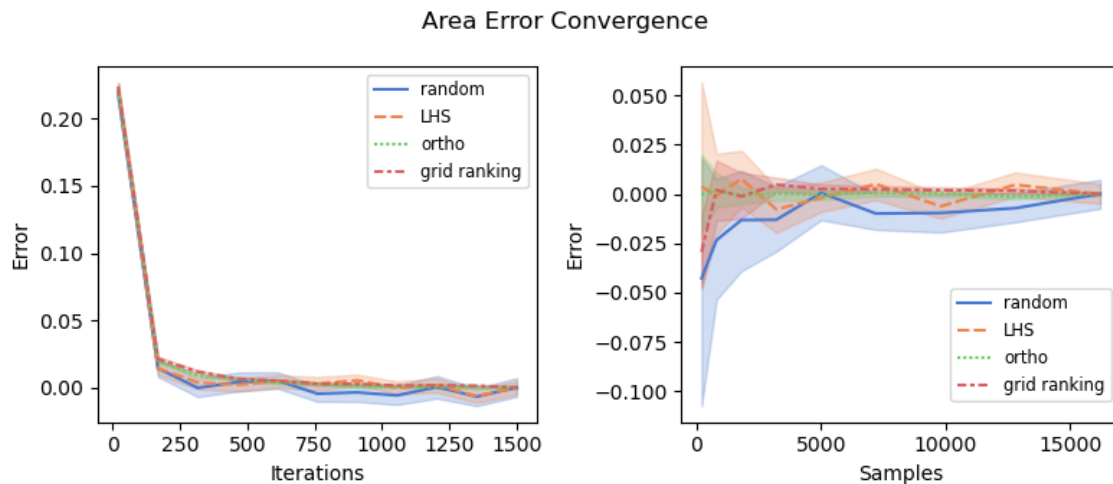


Figure 3: Convergence Area Error per method at 40 simulation runs. Left plot: iterations incrementally increased with samples fixed at 16200. Right plot: Sample sizes incrementally increased with iterations fixed at 150.

The quantity plotted in the cells is the resulting p-value. The left subplots depict the F-Tests, while the right subplots depict the T-Tests. Green indicates rejection of the null (p-value < 0.05), while red incites non-rejection of the null (p-value > 0.05).

F-test results From left subplots it can be observed that variances significantly differ between methods overall, regardless of increment of iteration or sample size, with some notable exceptions: the adaptive two-stage grid sampling (*gridrank*) does not have a significantly different variance when compared to Orthogonal Sampling for lower sample sizes, only at the maximum iteration and sample counts it has a significantly different variance. In some cases (iterations 612, 760 and sample sizes 200, 7200 and 12800) LHS variance does not differ significantly from random sampling and in at sample size = 1600 LHS variance does not differ significantly from *gridrank*.

T-test results From the right subplot it can be observed that the means generally do not significantly differ with some exceptions. differences in means seem to occur more frequently as same size increases from 7200 samples onward, with the iterations results supporting equality of means at iteration values 316 and 1352 for most methods. However, the pattern is not clear enough in either case to draw a clear conclusion about significant difference in means overall. This was expected from the plot where the mean values seem to vary in their overlapping regardless of setting for i and s .

Results at final Area Convergence Next we compare the distribution at the final convergence point, where $s = 16200$ and $i = 1500$. From figure 6 one can compare the distribution of area across simulation runs to the normal distribution with same mean and variance of that specific sample to adheres to the assumption of normality. The results are reasonable although we see some peaks diverging. With more simulation runs we would expect this result to improve.

Next we discuss can also observe the statistics at max convergence point in Table 1. The standard deviation is lower for each successive method with the lowest standard deviation obtained with the Adaptive Grid Rank sampling method. These differences are all significant as indicated in 5. The mean estimates differ slightly although, as indicated by the statistical tests, not significantly.

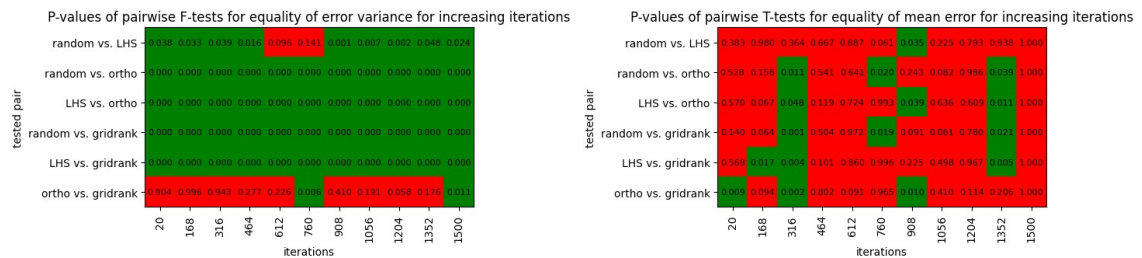


Figure 4: F-Test and T-Test results for increasing iterations. Green indicates rejection of the null hypothesis.

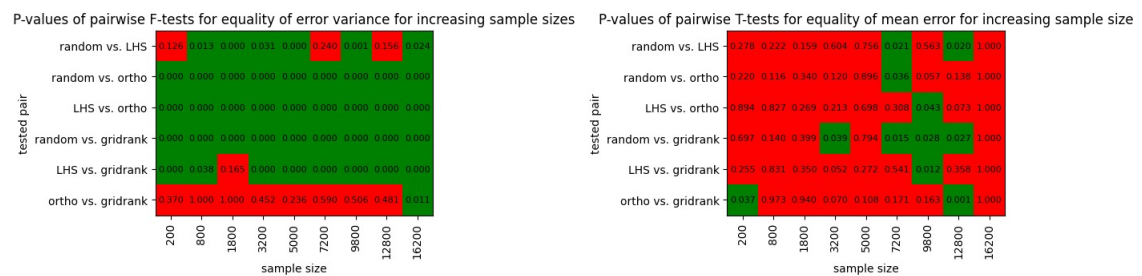


Figure 5: F-Test and T-Test results for increasing sample size. Green indicates rejection of the null hypothesis.

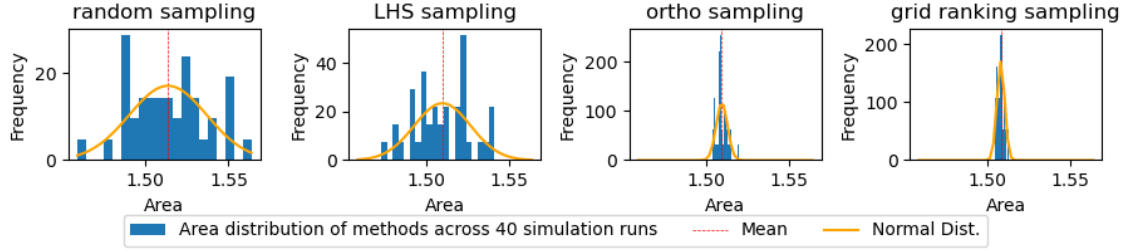


Figure 6: Distribution at max convergence at iterations = 1500 and samples = 16200 over 40 runs

Table 1: Summary of Sampling Types and Their Statistical Measures at max convergence

Sampling Type	Mean	Variance	Standard Deviation
Random	1.513519	0.000548	0.023399
LHS	1.509874	0.000288	0.016976
Ortho	1.509210	0.000012	0.003395
Grid Ranking	1.508256	0.000005	0.002344

Assumption Testing of statistical tests The T-test and F-test assume certain sample properties, namely, independent observations, normality, random sampling, and homogeneous sample variances. Independence of observation is ensured through random sampling in the Mandelbrot set, as prior observations don't influence subsequent observations. Normality is assumed based on the Central Limit Theorem and seems to approximately hold for the maximally converged area in Figure 6. The F-test's null hypothesis assumes equal variances, when testing against this assumption the F-Test reveals heterogeneous variances, for almost all settings of iterations and sample sizes, contradicting an assumption of the T-Test. Therefore, the Welch correction for unequal variances was applied to the T-test to account for that and improve reliability of results.

5 Discussion

The results exhibit a gradual increase in convergence rate with the increasing level of stratification. Whether the decrease in variance is concurrent with an approximation of the true area or is merely an artifact of the imposed spatial constraints remains a topic for further investigation, but from Table 1 it appears that all estimates except from the Pure Random Sampling come close to the findings outlined in the background literature.

At low sample sizes, Adaptive Grid Rank sampling shows greater mean error variability than orthogonal sampling, yet at higher sample sizes, its variance is half that of orthogonal sampling. This suggests potential greater efficiency for Adaptive Grid Rank sampling at large sample sizes, though further research is required.

The comparatively good performance of the adaptive sampling algorithm invites an investigation of further measures to improve its functionality. Due to the additional preliminary sampling step, the procedure generally takes longer to compute. Due to the different nature of the sampling distributions in the pre-sampling and the post-sampling stage, the first batch of samples is not included in the area calculations, but possibilities exist to "recycle" these in the secondary stage, as long as the observed Mandelbrot iterations are the same. Other improvements could include implementing orthogonal sampling in the second stage instead of LHS.

Furthermore, considering the recursive nature of the Mandelbrot fractal, a logical decision would be to integrate adaptive recursion in the sampling technique as well. Such techniques for Recursive Sampling have been found in literature[12] and can be seen as an extension of our two-step method into multiple temporal and spatial strata.

Popular techniques for variance reduction also include antithetic variables, control variates and importance sampling[9]. While investigating the applicability of these we noted several conclusions. First, antithetic variables producing negative covariance require the sampling of a monotonic function, which is not straightforward to define given the complex set structure.



The use of the symmetry correlation, however, let us reduce the search space and thus use more samples to obtain a certain precision. Second, a control variate could potentially be used which correlates the area estimate to the area of the enclosing circle of radius 2. The details for implementing this are a topic for future research. Finally, it could be argued that our two-stage sampling is a form of importance sampling, with the grid ranking defining the density distribution $g(x)$ which preconditions the preferential sampling in the secondary stage.

Concluding, our results show that increasing stratification progressively lowers the error variance, suggesting higher accuracy per unit compute and indicating that improvements beyond random Monte Carlo sampling are worth exploring for more efficient area estimation.

References

- [1] Benoit B Mandelbrot, Carl JG Evertsz, and Martin C Gutzwiller. *Fractals and chaos: the Mandelbrot set and beyond*. Vol. 3. Springer, 2004.
- [2] Adrien Douady and John H Hubbard. “Exploring the mandelbrot set. the orsay notes”. In: *Publ. Math. Orsay* (1984).
- [3] Mitsuhiro Shishikura. “The Hausdorff Dimension of the Boundary of the Mandelbrot Set and Julia Sets”. In: *Annals of Mathematics* 147.2 (1998), pp. 225–267. ISSN: 0003486X. URL: <http://www.jstor.org/stable/121009> (visited on 11/15/2023).
- [4] John H Ewing and Glenn Schober. “The area of the Mandelbrot set”. In: *Numerische Mathematik* 61.1 (1992), pp. 59–72.
- [5] Daniel Bittner et al. “New approximations for the area of the Mandelbrot set”. In: *Involve, a Journal of Mathematics* 10.4 (2017), pp. 555–572.
- [6] Ioannis Andreadis and Theodoros E. Karakasidis. “On numerical approximations of the area of the generalized Mandelbrot sets”. In: *Applied Mathematics and Computation* 219.23 (2013), pp. 10974–10982. ISSN: 0096-3003. DOI: <https://doi.org/10.1016/j.amc.2013.04.052>. URL: <https://www.sciencedirect.com/science/article/pii/S0096300313004876>.
- [7] A. C. Fowler and M. J. McGuinness. “The size of Mandelbrot bulbs”. In: *Chaos, Solitons & Fractals: X* 3 (2019), p. 100019. ISSN: 2590-0544. DOI: <https://doi.org/10.1016/j.csf.2019.100019>. URL: <https://www.sciencedirect.com/science/article/pii/S259005441930017X>.
- [8] Yuval Fisher and Jay Hill. “Bounding the area of the mandelbrot set”. In: *Availalbe at http://citeseer.ist.psu.edu/35134.html* (1993).
- [9] Sheldon M Ross. *Simulation*. Academic Press, 2022.
- [10] Stephen Leary, Atul Bhaskar, and Andy Keane. “Optimal orthogonal-array-based latin hypercubes”. In: *Journal of Applied Statistics* 30.5 (2003), pp. 585–598.
- [11] Kerry Mitchell. *A statistical investigation of the area of the mandelbrot set*. 2001.
- [12] William H Press and Glennys R Farrar. “Recursive stratified sampling for multidimensional Monte Carlo integration”. In: *Computers in Physics* 4.2 (1990), pp. 190–195.

A GitHub Statistics

The following excerpt was obtained using `git-fame` on the project repository <https://github.com/NitaiNijholt/StochSim>.

Author	loc	coms	fls	distribution
Boyan Mihaylov	2490191	50	44	99.9/67.6/91.7
NitaiNijholt	2727	16	3	0.1/ 21.6/ 5.3
VinayVardhan21	70	8	1	0.0/10.8/ 2.1
